J Appl Biomed
DOI: 10.32725/jab.2020.009
journal homepage: http://jab.zsf.jcu.cz

Journal of Applied Biomedicine

Original research article

Application of a neural interface for restoration of leg movements: Intra-spinal stimulation using the brain electrical activity in spinally injured rabbits

Mohamad Amin Younessi Heravi [1], Keivan Maghooli [1] *, Fereidoun Nowshiravan Rahatabad [1], Ramin Rezaee [2, 3]

[1] *Islamic Azad University, Science and Research Branch, Department of Biomedical Engineering, Tehran, Iran*
[2] *Mashhad University of Medical Sciences, Faculty of Medicine, Clinical Research Unit, Mashhad, Iran*
[3] *Mashhad University of Medical Sciences, Neurogenic Inflammation Research Center, Mashhad, Iran*

Abstract
This study aimed to design a neural interface that extracts movement commands from the brain to generate appropriate intra-spinal stimulation to restore leg movement. This study comprised four steps: (1) Recording electrocorticographic (ECoG) signals and corresponding leg movements in different trials. (2) Partial laminectomy to induce spinal cord injury (SCI) and detect motor modules in the spinal cord. (3) Delivering appropriate intra-spinal stimulation to the motor modules for restoration of the movements to those documented before SCI. (4) Development of a neural interface created by sparse linear regression (SLiR) model to detect movement commands transmitted from the brain to the modules. Correlation coefficient (CC) and normalized root mean square (NRMS) error was calculated to evaluate the neural interface effectiveness. It was found that by stimulating detected spinal cord modules, joint angle evaluated before SCI was not significantly different from that of post-SCI ($P > 0.05$). Based on results of SLiR model, overall CC and NRMS values were 0.63 ± 0.14 and 0.34 ± 0.16 (mean ± SD), respectively. These results indicated that ECoG data contained information about intra-spinal stimulations and the developed neural interface could produce intra-spinal stimulation based on ECoG data, for restoration of leg movements after SCI.

Keywords: Brain; Laminectomy; Linear models; Spinal cord stimulation

Highlights:
- Stimulating detected spinal cord modules before SCI was not significantly different.
- Stimulating joint angle evaluated before SCI was not significantly different.
- CNS commands delivered to the spinal cord, are more complicated than a simple pulse.

Introduction

Spinal cord injury (SCI) is one of the most common conditions of the nervous system which impairs impulse transmission from the brain to other organs. It is noteworthy that, SCI not only causes paralysis but also has a long-term impact on patient's quality of life and mental health (Duggan et al., 2016). The most important symptoms observed in subjects with SCI are muscular atrophy, joint stiffness, muscle spasms, osteoporosis and bedsores (Sezer et al., 2015). Studies done using functional magnetic resonance imaging (fMRI), indicated that even after SCI, the brain continues to generate electrical signals in response to an individual's intention to move (Freund et al., 2011). Also, it was indicated that electrophysiologic stimulation of the muscles, peripheral nerves, or spinal cord, below the level of injury, can lead to muscle activity (Jackson and Zimmermann, 2012). Such evidence offers a ray of hope in the treatment of SCI if we conceive paralysis as an information transfer lesion, where the information sent from the brain via the corticospinal tract, does not reach the spinal cord (Filli and Schwab, 2012). To restore limb function in individuals with SCI, this information transfer lesion must either be repaired or bypassed. To date, experimental efforts have focused on development of therapeutic approaches to repair the damaged spinal cord or prevent further damage after occurrence of the initial insult to the spinal cord (Hiebert et al., 2002). Transplantation of stem cells at the site of the injury, introduction of tissue-bridging biometrics and peripheral nerve transfers, and induction of neurotrophins and cytokines expression via viral transduction are examples of such approaches (Alam et al., 2016). Despite their great promise in the preclinical setting, these approaches showed limited success in clinical trials. The lack of an appropriate animal model of SCI, along with safety concerns associated with some of these therapeutic strategies, are cited as reasons for the poor translatability of

* **Author for correspondence:** Keivan Maghooli, Islamic Azad University, Science and Research Branch, Department of Biomedical Engineering, Ferdos Blvd 74, 1477893855,Tehran, Iran; e-mail: K-maghooli@srbiau.ac.ir
http://doi.org/10.32725/jab.2020.009
Submitted: 2020-05-01 • Accepted: 2020-06-12 • Prepublished online: 2020-06-26
J Appl Biomed 18/2–3: 33–40 • EISSN 1214-0287 • ISSN 1214-021X

these treatments in humans (Lobel and Lee, 2014; Rezaee and Abdollahi, 2017). Indeed, to date, there has been no report of restoration of limb movement following SCI at spinal level using neural interface technologies by electrical stimulators, to create a bypass around the SCI site (Cho et al., 2019; Freund et al., 2011).

Recent experiments confirmed efficacy of bypass using produced signals based on brain intention, to reanimate or mimic motor functions (Sharma et al., 2016). Generally, the neural interface inputs are signals extracted from intra-cortical microelectrodes (action potentials), electrocorticography (ECoG), or electroencephalography (EEG), and the outputs are signals used for direct stimulation of limbs and spinal cord (Caldwell et al., 2019). In the current study, we intended to obtain the required data for intra-spinal stimulation, from ECoG signals. It is known that the spinal cord of lower vertebrates has autonomous capabilities to produce basic coordinated patterns of locomotion in the absence of input from higher levels of the central nervous system or peripheral feedback (Nicolas-Alonso and Gomez-Gil, 2012). In this context, one of the recent approaches is controlling the movement at the level of the module in the spinal cord. Modular organization of spinally generated motor behaviors has been demonstrated in several experiments (Roh et al., 2011). These experiments documented that the vertebrate motor system produces movements by combining a small number of units of motor output (Ting et al., 2015). As a functional unit of the spinal cord, a module generates a particular motor output by inducing an explicit pattern (Bizzi et al., 2008). To functionalize paralyzed limbs, a proper pattern should be given to a module. An important challenge of restoring paralyzed motor function using bypass neural interface and intra-spinal stimulation, is generation of appropriate electrical stimulation patterns (Grahn et al., 2014). The aim of this study was to design an electrode-computer neural interface that extracts movement command from the brain to generate appropriate intra-spinal stimulation for restoring the leg movement. In this study, first, ECoG signals and corresponding leg movements were recorded in different trials. Following, surgical procedure was performed to induce SCI and detect motor modules in the spinal cord. Then, the appropriate intra-spinal stimulations were delivered to the motor modules for restoring the movements (i.e. to exert movements similar to those recorded before SCI induction). Finally, a neural interface was developed by sparse linear regression (SLiR) model to detect movement commands transmitted from the brain to the modules.

Materials and methods

Brain electrical activity and leg movement recording

This experimental study was done in the School of Medicine, North Khorasan University of Medical Sciences following the approval of the university ethics committee (IR.NKUMS.REC.1397.129). In this study, three male Dutch rabbits (weighing 1.63 ± 0.25 kg, 3.8 ± 0.55 months old) were used. All procedures were done in accordance with the national guidelines for animals' care and handling. Fig. 1 shows a schematic presentation of the experimental setup. First, electrodes were implanted in the bregma for ECoG recording. For this purpose, the rabbits were anesthetized using intraperitoneal ketamine hydrochloride (40 mg/kg; Alfasan, Holland) and xylazine hydrochloride (10 mg/kg; Pantex Holland B.V.). A custom-made electrode (diameter 0.40 mm) was implanted for signal recording. Two pairs of electrodes were implanted +1.0 cm from the bregma and 1 cm lateral to the midline and –2 cm from the bregma and 1 cm lateral to the midline. A ground electrode was placed under the neck skin. All materials were sealed and secured to the skull using dental cement, and the skin was sutured. One-week recovery was considered.

Then, animals were treated with chloroform through inhalation exposure to slow their fast activity. Animals were maintained in a position that allowed them to have free movements of the leg only. For evaluation of leg movement, the leg joints (i.e. hip, knee and ankle joints) were painted blue. To record a joint position, a digital camera that was located vertically above the right leg, was used. Using Microsoft visual studio (C#.Net software), real-time pictures (50 frames/second) were transferred to the computer and joint angles were identified by the colored indicator. In addition to joints angle in different movements, corresponding ECoG (sampling frequency 500 Hz) was recorded by the PowerLab system (ADInstruments, Australia).

Since the animals' legs were not laid on the ground, three-leg movements for intact rabbits (i.e. before laminectomy) were considered "before-injury movements (BIM)". The present work tried to restore these movements as all animals repeated them. BIM consisted of three main movements: Pushing leg to the back (the first BIM), Pulling the leg into the abdomen (the second BIM) and Pushing the leg forward (the third BIM). The leg movements in each BIM and corresponding ECoG signals were recorded 30–36 times for each animal. We defined "t" as the starting time point for each BIM when the animal moved its leg and corresponding ECoG was recorded 0.5 s before "t".

Surgical procedure

After signal recording, the rabbits were anesthetized using ketamine hydrochloride (40 mg/kg) and xylazine hydrochloride (10 mg/kg). To evaluate the cardiovascular system of the animals, electrocardiogram (ECG) signals in lead *I* were recorded by three Ag/AgCl electrodes (PowerLab system, AD Instrumentation Co., Australia). Next, a partial laminectomy was performed. Then, the spinal cord was exposed and fixed from T8 to L4 using two clips. During this experiment, the animal's leg movement did not affect the spinal cord position. For the induction of SCI, a complete transection of the spinal cord was done at the T7 vertebrae.

Module detection in the spinal cord

A custom-made stimulator equipped with eight isolated channels was designed to stimulate the spinal cord. This system was patented in the Iranian Patent Organization (Patent No. IRIPO100866) (Heravi et al., 2019). This device was connected to a computer and controlled by Microsoft visual studio C#.Net. The stimulation was induced by current pulses. Pulse shapes were single-phase and rectangular. Pulse amplitude, frequency and pulse width could be adjusted online. In the current study, the spinal cord was stimulated by pulses of constant frequency (50 Hz) and width (0.5 ms). To detect motor modules, the posterior horn of the spinal cord was stimulated. Firstly, electrodes were located at the T7 vertebrae, on the right of the spinal cord and entered (1 mm) into the spinal cord tissue. At this location, a constant current (150 μA) was delivered and the joint angles were monitored online. If following the stimulation, no movements were observed, then the electrodes were removed and located 2 mm further towards the neighboring vertebrae. To determine the best electrode position, this process was repeated towards the L4 vertebrae. Electrodes were fixed at the most appropriate position and the effect of stimulation amplitude on movement restoration was evaluated.

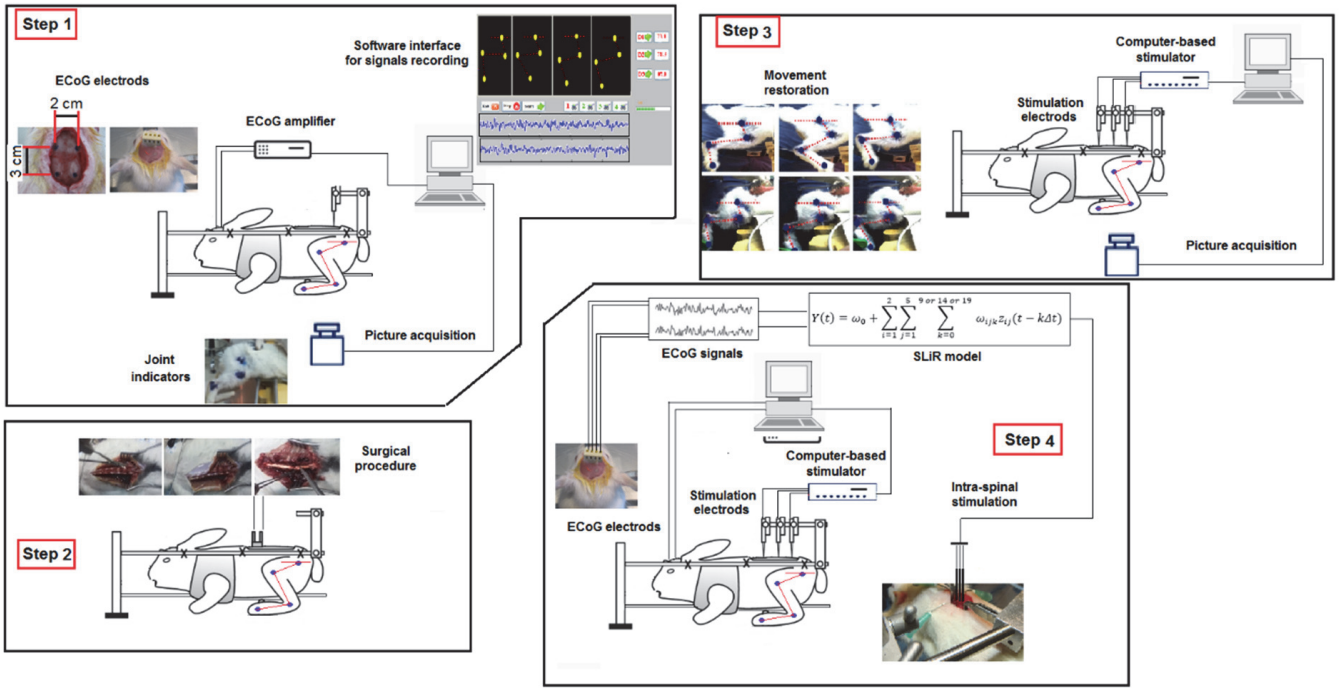

Fig. 1. Components of experimental setup

(**Step 1**) Preparation of the animals for the experiments and the signal recording; (**Step 2**) Surgical procedure for SCI induction and intra-spinal stimulation; (**Step 3**) Detection and activation of modules by intra-spinal stimulations for restoring movements based on trial-error process; (**Step 4**) Processing ECoG and designing the neural interface.

The effect of stimulation amplitude on movement is key to selecting stimulation patterns for inducing a particular movement. So, at each point where the electrode was inserted into the spinal cord, the stimulation patterns were obtained through a trial-and-error process to generate movements similar to the BIMs. The electrode location was considered appropriate if the relative error of joint angles was <10% (as calculated using Eq. 1). The electrodes were fixed to the vertebrae by using dental cement, and the skin was sutured. The diameter of stimulation electrodes was 0.4 mm. The rabbits were allowed to recover for one week. Here, three movements defined as "post-stimulation movements (PSMs)" were evaluated in laminectomized rabbits following intra-spinal stimulation. The three PSMs were: Pushing leg to the back (the first PSM); Pulling the leg into the abdomen (the second PSM) and Pushing the leg forward (the third PSM) The relative error of joint angles was calculated using the Eq. 1:

$$\%Relative\ error\ of\ joint\ angle = \frac{\theta_{BIM}(t) - \theta_{PSM}(t)}{\theta_{BIM}(t)} * 100$$

(Eq. 1)

Where θ_{BIM} and θ_{PSM} are the joint angles before the injury and after stimulation, respectively. The diameter of stimulation electrodes was 0.4 mm.

By combining the appropriate intra-spinal stimulation and inducing the three detected motor modules, restoration of leg movements was performed. Each experiment was repeated 10 times for each rabbit. Joint angles were recorded in the first state (i.e. BIMs) and after induction of a combination of three intra-spinal stimulations (i.e. PSMs). Normalized Root Mean Square (NRMS) error of tracking was calculated to measure the tracking performance as follows (Eq. 2):

$$NRMS = \frac{\sqrt{\sum_{i=1}^{n} \left(y_i^{predicted} - y_i^{actual}\right)^2 / n}}{\left(y_{max}^{actual} - y_{min}^{actual}\right)}$$

(Eq. 2)

For each performance i, $y_i^{predicted}$ and y_i^{actual} are the joint angle before the injury (θ_{BIM}) and after stimulation (θ_{PSM}), y_{max}^{actual} and y_{min}^{actual} are the maximum and minimum of θ_{BIM}, and n is the total time considered in the movement restoration process. The similarity of joint angles in the first state and after intra-spinal stimulations was evaluated by calculation of the correlation coefficient (CC).

Processing brain electrical activity and designing a neural interface

After finding the appropriate intra-spinal stimulation, a neural interface was developed using a SLiR model to predict intra-spinal stimulations using the ECoG signals. The SLiR efficiently and automatically selected fitting parameters to achieve an enhanced overview of performance over that gained from other ordinary linear regression models (Chen et al., 2013; Nakanishi et al., 2014, 2017). The inputs of the neural interface were extracted from the ECoG signal and the outputs were amplitude current of intra-spinal stimulations required for restoring the PSMs.

In the beginning, preprocessing was performed by a common average reference on raw ECoG signals. The common average reference method calculates the mean of two channels and subtracts the average value of two channels from the values of each selected channel. This method increases the signal-to-noise ratio (Ludwig et al., 2009; McFarland et al., 1997).

Subsequently, the signal was divided into five frequency bands by bidirectional fourth-order Butterworth band-pass filters. For each ECoG signal, five frequency bands: δ, θ, α, β, and γ that ranged from ~4, 4~8, 8~14, 14~30, and 30~50 Hz respectively, were considered. These specific frequency bands were considered as they are commonly used in current ECoG based brain-computer interface studies (Shin et al., 2012). Next, these band-passed signals were digitally rectified and smoothed using a second-order low-pass filter. High oscillations of each frequency band were changed into low. The cut-off frequency of low pass filter was 2.2 Hz (Nakanishi et al., 2013). After that, the sampling frequency signals were reduced to 50 Hz based on the sampling frequency intra-spinal stimulations. Finally, each smoothed signal $x_i(t)$ at time t was z-score normalized to produce the final ECoG features $z_i(t)$, using Eq. 3 (Shin et al., 2018):

$$z_{ij}(t) = \frac{x_{ij}(t) - \mu_{ij}}{\sigma_{ij}}$$

(Eq. 3)

where, i and j are the electrode channel and the frequency band, respectively. μ_{ij} and σ_{ij} denote the mean value and the standard deviation of $x_{ij}(t)$ over a "T" interval before time t, respectively. $z_{ij}(t)$ in the "T" interval became the final ECoG feature used in intra-spinal stimulation prediction. These z-scores calculated from ECoG signals were utilized as training data to construct a model. We also examined the weights of the prediction model to infer which sensorimotor rhythms contribute more to the prediction. The amplitude stimulation at time t, $Y(t)$, was decoded using the ECoG feature signal $z_{ij}(t)$ over a "T" second interval before time t (Eq. 4):

$$Y_p(t) = \omega_0 + \sum_{i=1}^{2}\sum_{j=1}^{5}\sum_{k=0}^{9\ or\ 14\ or\ 19\ or\ 24} \omega_{ijk} z_{ij}(t - k\Delta t)$$

(Eq. 4)

where p represents the predicted value of each stimulation signal, Δt is 20 ms, ω_{ijk} is the weights according to the ECoG feature signal $z_{ij}(t)$ at electrode channel i, frequency band j, and time $t - k\Delta t$, and ω_0 is the bias. SparseReg MATLAB toolbox (Gaines et al., 2018) was used to determine model parameters and values of the weights. Validity of the method was examined by Leave One Out cross-validation. First, based on ECoG signals and corresponding intra-spinal stimulation, a model was developed in all experiments except for the kth trial, that was employed as test data. The weight coefficients were achieved from this training. Iterations of the sparse linear regression were ended just before over-training. Moreover, an intra-spinal stimulation Y_p in the kth trial was predicted using the constructed model. CC and the NRMS error were obtained by comparing Y_p and Y_{act} of the kth test trial. Also, the above-mentioned training and testing phases were repeatedly executed using different trials for k. Finally, the CC and NRMS values were averaged across all trials. NRMS error was calculated based on Eq. 2. For each time i, $y_i^{predicted}$ is the predicted intra-spinal stimulation, y_i^{actual} is the actual intra-spinal stimulation, and y_{max}^{actual} and y_{min}^{actual} are the maximum and minimum of actual intra-spinal stimulations, respectively, and n is the total time. CC and NRMS were considered prediction performance of neural interface that was calculated by MATLAB software version 2011a. We also applied the prediction model to restore the movements in real-time conditions and the performance of the model was then evaluated. The real-time data acquisition and processing were performed by MATLAB SIMULINK, Real-Time Workshop and Real-Time Windows Target. The models were implemented by the S-functions and synchronized by Microsoft visual studio.

Statistical analysis

The joint angles in BIMs and PSMs were analyzed by the t-test. Also, the ANOVA followed by Tukey's multiple-comparison test, was adopted to analyze the effects of different parameters on the predictive performance of the neural interface. All statistical analysis was performed by SPSS version 16. A $p < 0.05$ was considered significant.

Results

In this study, three motor modules were stimulated in the spinal cord and three leg movements (i.e. PSM 1, 2 and 3) were evaluated following intra-spinal stimulations by measuring joint angles.

The results of spinal cord stimulations showed that in the first PSM (i.e. backward pushing of the leg), activation locations varied among the rabbits, but generally they were located at L2–L5. The stimulation threshold was 87.5 ± 4.51 μA. The second PSM (i.e. pulling the leg towards the abdomen) was obtained by stimulation at T13–L1. The stimulation threshold was 105.4 ± 8.20 μA. The third PSM (i.e. forward pushing of the leg), was induced by an electric current of 89.3 ± 6.23 μA delivered at L1–L3. Electrode location varied among the animals but all were located on the right of the spinal cord and at a depth of >1 mm. The effect of stimulation amplitude on movements showed that by increasing the pulse amplitude, the movement of each joint increased. It is noteworthy that a minimum pulse amplitude (i.e. threshold) was required to restore each movement. Fig. 2 shows three joint angles in the first step and after intra-spinal stimulation.

The t-test analysis of joint angles showed that there were no significant differences between joint angles in BIMs and PSMs ($p < 0.05$). Based on our data, using a combination of three recognized intra-spinal stimulations, mean (SD) of CC and NRMS error of tracking were respectively 0.69 ± 0.127 and 0.34 ± 0.117 (for rabbit 1,2), 0.67 ± 0.124 and 0.38 ± 0.213 (for rabbit 2), 0.66 ± 0.232 and 0.33 ± 0.215 (for rabbit 3). The CC, mean (SD) for the 3 rabbits (10 trials each), was 0.69 ± 0.122, 0.68 ± 0.225 and 0.66 ± 0.204 for the hip, knee, and ankle, respectively. The NRMS error of tracking, mean (SD) for the 3 rabbits (10 trials each), were also calculated 0.36 ± 0.126, 0.34 ± 0.215, and 0.41 ± 0.135 for the hip, knee, and ankle, respectively.

Movement duration average and standard deviations of 30 trials for the 1st, 2nd and 3rd PSM were 0.46 ± 0.24, 0.53 ± 0.23 and 0.41 ± 0.19, respectively. It was found that the movements of each trial were non-uniform. The effect of the different T intervals, each individual ECoG electrode, and each sensorimotor rhythm on predictive performance is shown in Fig. 3. The effect of the T interval on ECoG processing was assessed using both ECoG channels 1 and 2 and all sensorimotor rhythms. The 2-way ANOVA showed a significantly better performance by using 200 ms (for rabbit 3) and 300 ms (for rabbits 1, 2) compared to other T intervals [CC: F (3,348) = 3.074, P = 0.0364, and NRMS: F (3,348) = 3.491, P = 0.0155]. The intra-spinal stimulation was predicted using each ECoG electrode position individually by the best T interval and all sensorimotor rhythms. The 2-way ANOVA showed that per-

formance using both ECOG channels (i.e. channel 1 and 2) was significantly better than others in all animals [CC: F (2,171) = 4.290, P = 0.032, and NRMS: F (2,171) = 5.074, P = 0.026]. The 2-way ANOVA of each sensorimotor rhythm showed that the CC values of the δ and γ bands were significantly higher compared to the other bands [F (4,435) = 4.19 P = 0.017]. Also, the γ band performance was significantly weaker compared to the other bands in all animals [F (4,435) = 3.491, P = 0.0185]. Moreover, there were significant differences between all sensorimotor rhythms and each specific rhythm in CC and NRMS error [F (5,552) = 3.26 P = 0.0115] and [F (5,552) = 2.16 P = 0.0169].

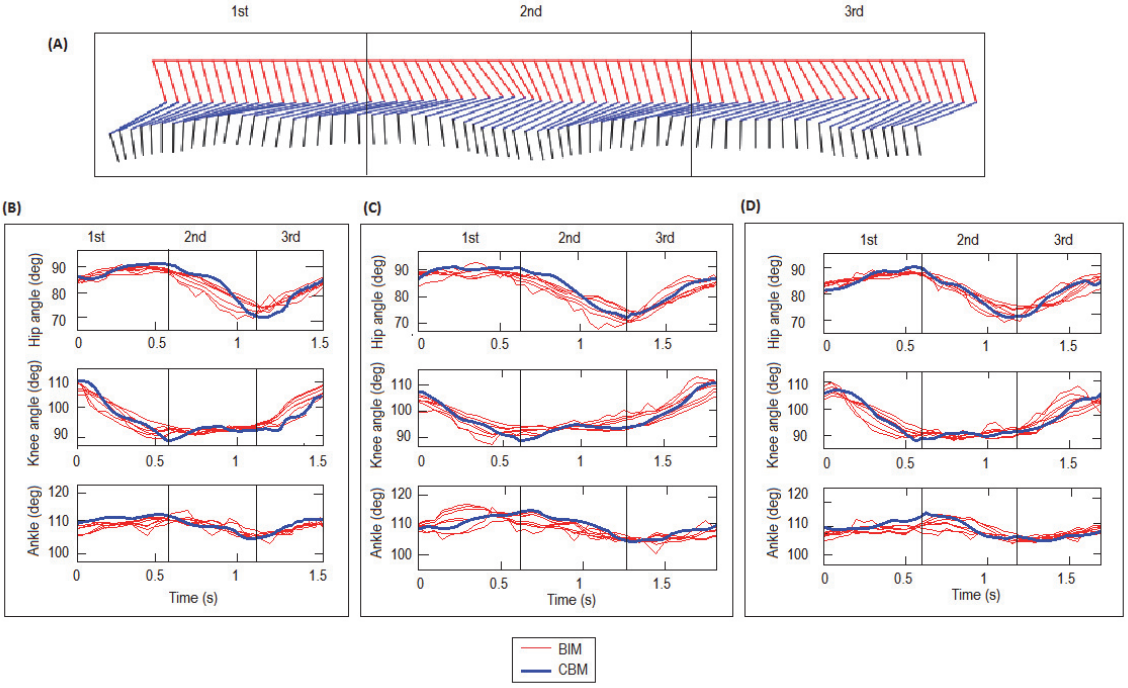

Fig. 2. Changes in joint angles in the first step and after intra-spinal stimulation
(**A**) Variations of joint angles. (**B**), (**C**) and (**D**) indicate the 3 joint angles for the BIMs and PSMs in rabbit 1, 2, and 3 respectively. The blue and red lines show joint angles variations over time in BIMs and PSMs. In the first PSM, the hip and ankle joint angles increased while the knee joint angles decreased. In the second PSM, the knee joint angle increased but the hip and ankle joint angles decreased. In the third PSM, all joint angles increased.

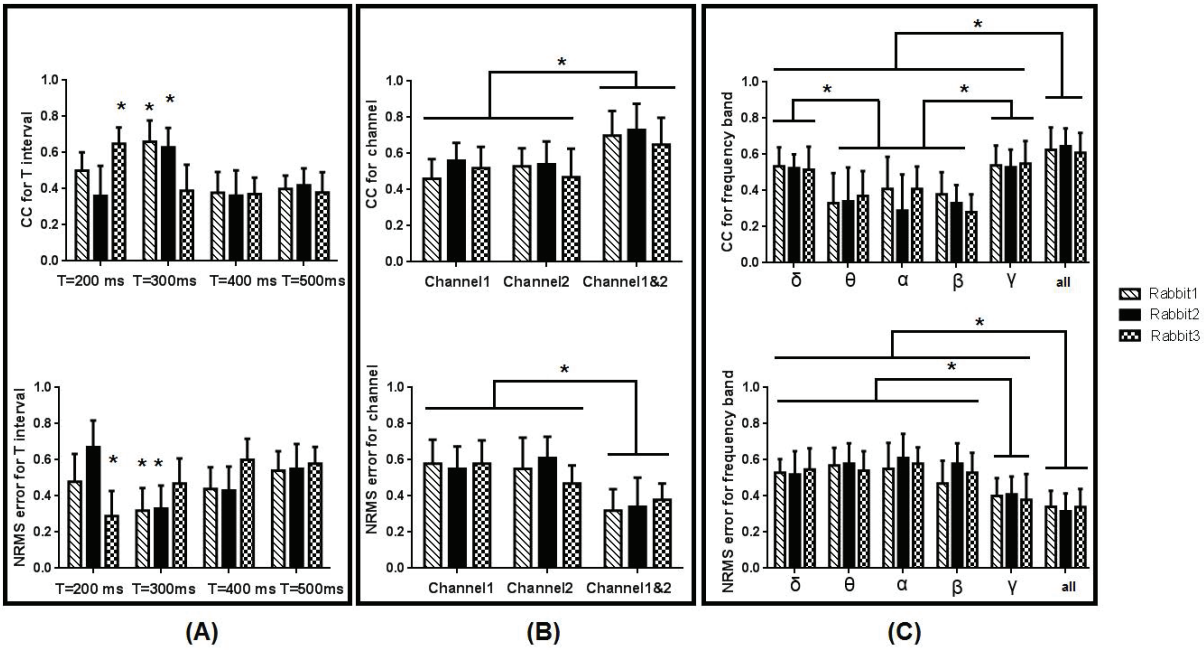

Fig. 3. The results of predictive performance
(**A**) CC and NRMS error for different T; (**B**) CC and NRMS error for application of channel 1, channel 2 and channel 1 and 2 of ECoG; (**C**) CC and NRMS error for different sensorimotor rhythms. Significant differences at $p < 0.05$ between different parameters are marked with *. CC and NRMS error are shown as mean ± standard deviation of 30 experiments (ten for each rabbit).

Fig. 4 shows an example of ECoG features extraction and the predicted intra-spinal stimulation by SLiR model that generated PSMs during a trial by rabbit 1. The figure shows that the predicted intra-spinal stimulation by SLiR model fit the intra-spinal stimulations required for restoring the PSMs.

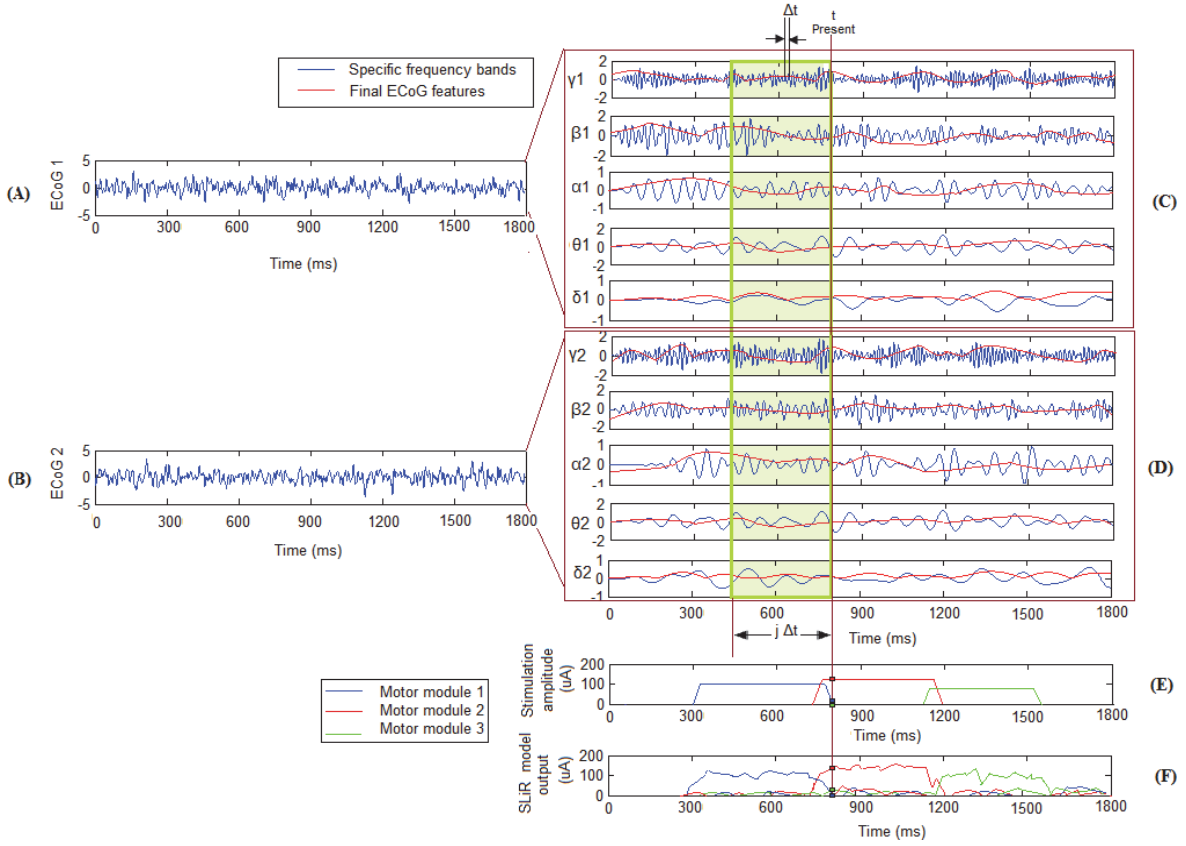

Fig. 4. Processing the ECoG signals and prediction of intra-spinal stimulation by SLiR model
(**A**) and (**B**) show the raw ECoG obtained by PowerLab in 2 channels; (**C**) and (**D**) show five frequency bands for 2 channels; (**E**) illustrates corresponding intra-spinal stimulation and (**F**) presents the predicted intra-spinal stimulation by SLiR model.

Table 1 shows the results of predictive performance. The best CC and NRMS error for intra-spinal stimulations were 0.70 ± 0.148 and 0.27 ± 0.098 respectively. One-way ANOVA was used to identify significant differences in predictive performances among test subsets. For each rabbit, no significant differences in CC [F (9,290) = 0.36, P = 0.89] and NRMS [F (9,290) = 0.25, P = 0.96] were observed among 10 test subsets.

Table 1. Prediction performance of neural interface in 10 test subsets

Test data	Rabbit 1 1st = L2, 2nd = T13, 3rd = L1 T = 300 ms		Rabbit 2 1st = L2, 2nd = L1, 3rd = L1 T = 300 ms		Rabbit 3 1st = L3, 2nd = L1, 3rd = L2 T = 200 ms	
	CC	NRMS	CC	NRMS	CC	NRMS
1	0.68 ± 0.181	0.36 ± 0.125	0.62 ± 0.281	0.33 ± 0.127	0.53 ± 0.181	0.40 ± 0.145
2	0.66 ± 0.176	0.34 ± 0.185	0.66 ± 0.166	0.38 ± 0.096	0.65 ± 0.176	0.35 ± 0.259
3	0.66 ± 0.159	0.36 ± 0.152	**0.69 ± 0.106**	0.27 ± 0.095	0.66 ± 0.159	0.29 ± 0.176
4	**0.70 ± 0.148**	**0.29 ± 0.084**	0.67 ± 0.094	0.31 ± 0.169	0.67 ± 0.248	**0.28 ± 0.117**
5	0.68 ± 0.124	0.35 ± 0.113	0.60 ± 0.078	0.35 ± 0.094	0.61 ± 0.124	0.38 ± 0.112
6	0.64 ± 0.093	0.34 ± 0.157	0.67 ± 0.163	**0.27 ± 0.098**	**0.68 ± 0.093**	0.29 ± 0.152
7	0.64 ± 0.282	0.32 ± 0.159	0.61 ± 0.124	0.33 ± 0.126	0.62 ± 0.282	0.37 ± 0.088
8	0.59 ± 0.174	0.38 ± 0.094	0.66 ± 0.098	0.31 ± 0.088	0.58 ± 0.174	0.40 ± 0.091
9	0.66 ± 0.079	0.44 ± 0.081	0.67 ± 0.077	0.29 ± 0.096	0.66 ± 0.179	0.38 ± 0.117
10	0.57 ± 0.181	0.32 ± 0.159	0.65 ± 0.081	0.34 ± 0.218	0.59 ± 0.181	0.39 ± 0.210
Mean ± SEM	0.64 ± 0.159	0.35 ± 0.130	0.65 ± 0.126	0.30 ± 0.120	0.62 ± 0.179	0.35 ± 0.146

1st, represents the location of stimulation in the first PSM. 2nd, represents the location of stimulation in the second PSM. 3rd, represents the location of stimulation in the third PSM. The bold values show the best results. CC, correlation coefficient and NRMS: normalized root mean square.

Fig. 5 shows an example of real-time restoration of movements in spinally-injured rabbit. For real-time evaluation of the process, the joint angles before SCI and corresponding stimulation signals that led to these joint angles, were considered "actual values of joint angles" and "intra-spinal stimulations", respectively.

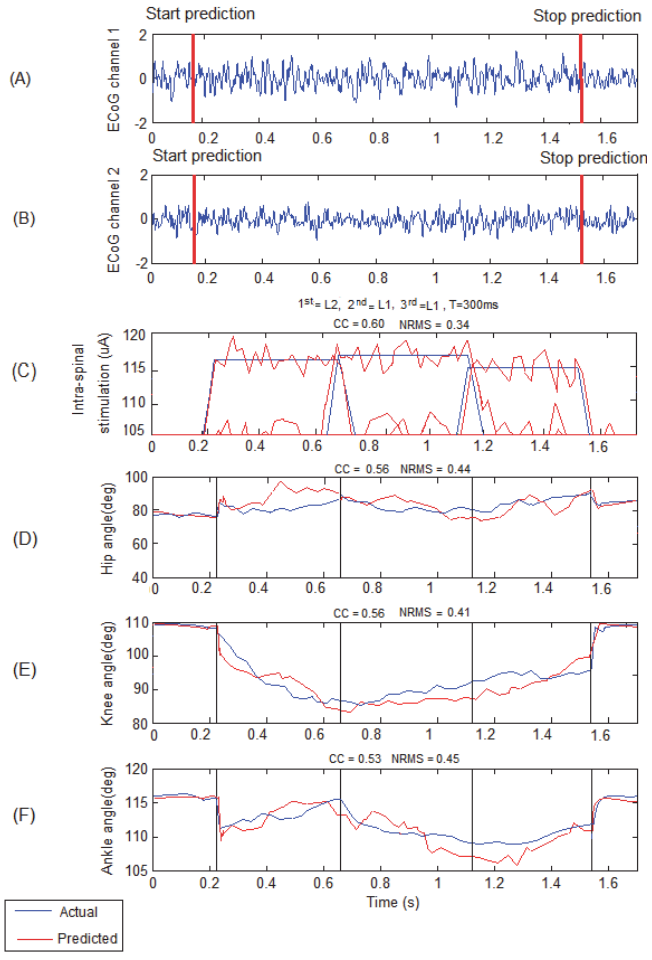

Fig. 5. Real-time restoring leg movements in a spinally-injured rabbit by the SLiR model

(**A**) Channel 1 and (**B**) channel 2 ECoG recording; (**C**) prediction and actual intra-spinal stimulation (**D**); (**E**) and (**F**) respectively show hip, knee, and ankle joint angles, in three PSMs, as "actual" and three real-time restored joint angles as "restored".

The performance of real-time restoration of movements ranged from 0.41 to 0.60 and from 0.25 to 0.48 based on CC and NRMS, respectively. These results clearly showed that the model could predict intra-spinal stimulation based on ECoG and the PSMs were restored by predicted intra-spinal stimulation with appropriate performance.

Discussion

In this study, an ECoG-based model was developed for induction of intra-spinal stimulation prediction for restoring monitored movements. The results of module detection showed that by stimulating detected spinal cord modules, joint angles evaluated in BIMs were not significantly different from those of PSMs ($P > 0.05$). So, electrical stimulation of the spinal cord modules was found helpful in restoration of leg movements in laminectomized rabbits. The overall CC and NRMS calculated for joint angle were respectively 0.67 ± 0.21 and 0.34 ± 0.11. It indicated acceptable tracking performance in leg movement's restoration. The results of application of the present neural interface showed that the overall (mean ± SEM of 10 trials for each of the three rabbits) CC and NRMS values were 0.63 ± 0.14 and 0.34 ± 0.16, respectively. These results indicated that ECoG data contained information about intra-spinal stimulations and the neural interface could predict intra-spinal stimulation based on ECoG for restoring PSMs. The results of real-time restoration of movements using SLiR model showed overall CC and NRMS error tracking of 0.51 ± 0.09 and 0.46 ± 0.09, respectively. The CC and NRMS values showed weaker performance compared to the non-real-time process, but these values were achieved based on real-time prediction and showed approximately appropriate results. The results of spinal cord electrical stimulation showed that stimulation of upper vertebrae, T13 to L1, leads to joints closing while stimulation of the spinal circuitry of the next vertebrae leads to joints opening which is in line with results reported by previous studies (Aasdi and Erfanian Omidvar, 2013; Righetti and Ijspeert, 2006). In the present work, the range of each movement increased with increasing stimulation amplitude.

The results of neural interface performance using one or two-channel ECoG analysis showed that predictive performance was improved by ECoG processing of two channels. This indicates that, using higher numbers of ECoG channels might improve predictive results. In this study, the results of performance for frequency band showed that the γ and δ bands significantly affected CC compared to the other bands while on NRMS error, only γ bands had significant effect. In ECoG-based BMIs studies, the γ rhythm has been widely used (Pistohl et al., 2008; Yanagisawa et al., 2012). Several articles also reported that γ rhythm was useful for 3D hand trajectory (Shimoda et al., 2012) and EMG prediction (Shin et al., 2012) in monkeys. Also, some reports indicated that the δ and γ bands were suitable for decoding arm motion (Chao et al., 2010), arm movement trajectories (Pistohl et al., 2008), grasp force profile (Chen et al., 2013), joint angle and muscle activity (Shin et al., 2018) based on the ECoG. Our results are in good agreement with the previous reports (Chao et al., 2010; Chen et al., 2013; Shin et al., 2012, 2018). Although we identified the ECoG frequency bands with the highest performance, the best overall performance was achieved when all sensorimotor rhythms were considered. This might indicate that all sensorimotor rhythms of ECoG encode modules activity in the spinal cord and therefore, they are required, at least to some degree, to predict such activities.

Body weight is an important issue in movement restoring studies. Thus, body weight should be considered if there is a gait pattern for evaluation of intensity rate and pulse stimulation variables. Several kinds of modules depending on muscle pattern and/or force pattern changes were defined in the literature (Bizzi et al., 2008; Tresch et al., 2002). Here, we defined the modules based on the changes in recorded joint angle as we wanted to restore BIMs and evaluate these movements based on joint angles. To activate each module, we delivered electrical stimulation to the spinal cord module. However, the trial-and-error method is a time-consuming inefficient approach for generating stimulation patterns.

Conclusions

The results of present study indicated which intra-spinal stimulations and the developed neural interface could produce intra-spinal stimulation based on ECoG data, for restoration of leg movements after SCI.

It should be noted that future studies that may employ the present approach for restoring movements should consider body weight. Since electromyography (EMG) analysis of leg movements could improve the results, it is recommended to be considered in future studies.

Conflict of interests

The authors have no conflict of interests to declare.

References

Aasdi A, Erfanian Omidvar A (2013). Restoring the Stepping-Like Movement in Spinal Rat by Electrical Micro-Stimulation of Motor Primitive Blocks. J Isfahan Med School 31: 1324–1328.

Alam M, Rodrigues W, Pham BN, Thakor NV (2016). Brain-machine interface facilitated neurorehabilitation via spinal stimulation after spinal cord injury: Recent progress and future perspectives. Brain Res 1646: 25–33. DOI: 10.1016/j.brainres.2016.05.039.

Bizzi E, Cheung VCK, d'Avella A, Saltiel P, Tresch M (2008). Combining modules for movement. Brain Res Rev 57: 125–133. DOI: 10.1016/j.brainresrev.2007.08.004.

Caldwell DJ, Ojemann JG, Rao RP (2019). Direct Electrical Stimulation in Electrocorticographic Brain-Computer Interfaces: Enabling Technologies for Input to Cortex. Front Neurosc 13: 804. DOI: 10.3389/fnins.2019.00804.

Chao ZC, Nagasaka Y, Fujii N (2010). Long-term asynchronous decoding of arm motion using electrocorticographic signals in monkey. Front Neuroeng 3: 3. DOI: 10.3389/fneng.2010.00003.

Chen C, Shin D, Watanabe H, Nakanishi Y, Kambara H, Yoshimura N, et al. (2013). Prediction of hand trajectory from electrocorticography signals in primary motor cortex. PloS One 8. DOI: 10.1371/journal.pone.0083534.

Cho N, Squair JW, Bloch J, Courtine G (2019). Neurorestorative interventions involving bioelectronic implants after spinal cord injury. Bioelectron Med 5: 10. DOI: 10.1186/s42234-019-0027-x.

Duggan C, Wilson C, Diponio L, Trumpower B, Meade MA (2016). Resilience and happiness after spinal cord injury: a qualitative study. Top Spinal Cord Inj Rehabil 22: 99–110. DOI: 10.1310/sci2202-99.

Filli L, Schwab ME (2012). The rocky road to translation in spinal cord repair. Ann Neurol 72: 491–501. DOI: 10.1002/ana.23630.

Freund P, Weiskopf N, Ward NS, Hutton C, Gall A, Ciccarelli O, et al. (2011). Disability, atrophy and cortical reorganization following spinal cord injury. Brain 134: 1610–1622. DOI: 10.1093/brain/awr093.

Gaines BR, Kim J, Zhou H (2018). Algorithms for fitting the constrained lasso. J Comput Graph Stat 27: 861–871. DOI: 10.1080/10618600.2018.1473777.

Grahn PJ, Mallory GW, Berry BM, Hachmann JT, Lobel DA, Lujan JL (2014). Restoration of motor function following spinal cord injury via optimal control of intraspinal microstimulation: toward a next generation closed-loop neural prosthesis. Front Neurosci 8: 296. DOI: 10.3389/fnins.2014.00296.

Heravi MAY, Maghooli K, Rahatabad FN, Rezaee R (2019). Intra-Spinal Stimulation Leads to Activation of Motor Modules and Restoration of Monitored Movements in Spinally-Injured Rabbits. NeuroQuantology 17: 71–79. DOI: 10.14704/nq.2019.17.6.2456.

Hiebert G, Khodarahmi K, McGraw J, Steeves J, Tetzlaff W (2002). Brain-derived neurotrophic factor applied to the motor cortex promotes sprouting of corticospinal fibers but not regeneration into a peripheral nerve transplant. J Neurosci Res 69: 160–168. DOI: 10.1002/jnr.10275.

Jackson A, Zimmermann JB (2012). Neural interfaces for the brain and spinal cord – restoring motor function. Nat Rev Neurol 8: 690. DOI: 10.1038/nrneurol.2012.219.

Lobel DA, Lee KH (2014). Brain machine interface and limb reanimation technologies: Restoring function after spinal cord injury through development of a bypass system. Mayo Clin Proc 89: 708–714. DOI: 10.1016/j.mayocp.2014.02.003.

Ludwig KA, Miriani RM, Langhals NB, Joseph MD, Anderson DJ, Kipke DR (2009). Using a common average reference to improve cortical neuron recordings from microelectrode arrays. J Neurophysiol 101: 1679–1689. DOI: 10.1152/jn.90989.2008.

McFarland DJ, McCane LM, David SV, Wolpaw JR (1997). Spatial filter selection for EEG-based communication. Electroencephalogr Clin Neurophysiol 103: 386–394. DOI: 10.1016/s0013-4694(97)00022-2.

Nakanishi Y, Yanagisawa T, Shin D, Chen C, Kambara H, Yoshimura N, et al. (2014). Decoding fingertip trajectory from electrocorticographic signals in humans. Neurosci Res 85: 20–27. DOI: 10.1016/j.neures.2014.05.005.

Nakanishi Y, Yanagisawa T, Shin D, Fukuma R, Chen C, Kambara H, et al. (2013). Prediction of three-dimensional arm trajectories based on ECoG signals recorded from human sensorimotor cortex. PloS One 8. DOI: 10.1371/journal.pone.0072085.

Nakanishi Y, Yanagisawa T, Shin D, Kambara H, Yoshimura N, Tanaka M, et al. (2017). Mapping ECoG channel contributions to trajectory and muscle activity prediction in human sensorimotor cortex. Sci Rep 7: 45486. DOI: 10.1038/srep45486.

Nicolas-Alonso LF, Gomez-Gil J (2012). Brain computer interfaces, a review. Sensors 12: 1211–1279. DOI: 10.3390/s120201211.

Pistohl T, Ball T, Schulze-Bonhage A, Aertsen A, Mehring C (2008). Prediction of arm movement trajectories from ECoG-recordings in humans. J Neurosci Methods 167: 105–114. DOI: 10.1016/j.jneumeth.2007.10.001.

Rezaee R, Abdollahi M (2017). The importance of translatability in drug discovery. Expert Opin Drug Discov 12: 237–239. DOI: 10.1080/17460441.2017.1281245.

Righetti L, Ijspeert AJ (2006). Programmable central pattern generators: an application to biped locomotion control. Proceedings IEEE International Conference on Robotics and Automation, 2006. ICRA 2006. IEEE 1585–1590. DOI: 10.1109/ROBOT.2006.1641933.

Roh J, Cheung VC, Bizzi E (2011). Modules in the brain stem and spinal cord underlying motor behaviors. J Neurophysiol 106: 1363–1378. DOI: 10.1152/jn.00842.2010.

Sezer N, Akkuş S, Uğurlu FG (2015). Chronic complications of spinal cord injury. World J Orthop 16: 24–33. DOI: 10.5312/wjo.v6.i1.24.

Sharma G, Friedenberg DA, Nicholas A, Bradley G, Bockbrader M, Majstorovic C, et al. (2016). Using an artificial neural bypass to restore cortical control of rhythmic movements in a human with quadriplegia. Sci Rep 6: 33807. DOI: 10.1038/srep33807.

Shimoda K, Nagasaka Y, Chao ZC, Fujii N (2012). Decoding continuous three-dimensional hand trajectories from epidural electrocorticographic signals in Japanese macaques. J Neural Eng 9: 036015. DOI: 10.1088/1741-2560/9/3/036015.

Shin D, Kambara H, Yoshimura N, Koike Y (2018). Control of a Robot Arm Using Decoded Joint Angles from Electrocorticograms in Primate. Comput Intel Neurosc 2018: 1–8. DOI: 10.1155/2018/2580165.

Shin D, Watanabe H, Kambara H, Nambu A, Isa T, Nishimura Y, Koike Y (2012). Prediction of muscle activities from electrocorticograms in primary motor cortex of primates. PloS One 7(10): e47992. DOI: 10.1371/journal.pone.0047992.

Ting LH, Chiel HJ, Trumbower RD, Allen JL, McKay JL, Hackney ME, Kesar TM (2015). Neuromechanical principles underlying movement modularity and their implications for rehabilitation. Neuron 86: 38–54. DOI: 10.1016/j.neuron.2015.02.042.

Tresch MC, Saltiel P, d'Avella A, Bizzi E (2002). Coordination and localization in spinal motor systems. Brain Res Rev 40: 66–79. DOI: 10.1016/s0165-0173(02)00189-3.

Yanagisawa T, Hirata M, Saitoh Y, Kishima H, Matsushita K, Goto T, et al. (2012). Electrocorticographic control of a prosthetic arm in paralyzed patients. Ann Neurol 71: 353–361. DOI: 10.1002/ana.22613.